

## **Supporting Information**

### **Synthesis, Structures and Photophysical Properties of Tetra- and Hexanuclear Zinc-Hydroxido-Acetato-Clusters Supported by Tridentate Salicylaldiminato Ligands**

**Tobias Severin,<sup>a</sup> Viktoriia Karabtsova,<sup>a</sup> Martin Börner,<sup>a</sup> Hendrik Weiske,<sup>b</sup> Agnieszka Kuc,<sup>c</sup> and Berthold Kersting,<sup>a,\*</sup>**

#### **Content**

1. Characterization of compounds - Infrared spectroscopy.
2. Packing diagram for **HL**.
3. Determination of Coordination Geometries utilizing SHAPE.
4. Characterization of compounds - NMR spectroscopy
5. Characterization of compounds - UV/vis spectroscopy & Fluorescence spectroscopy
6. Characterization of compounds - DFT calculations
7. Characterization of compounds - Determination of LOD values

## 1. Characterization of compounds - Infrared Spectroscopy

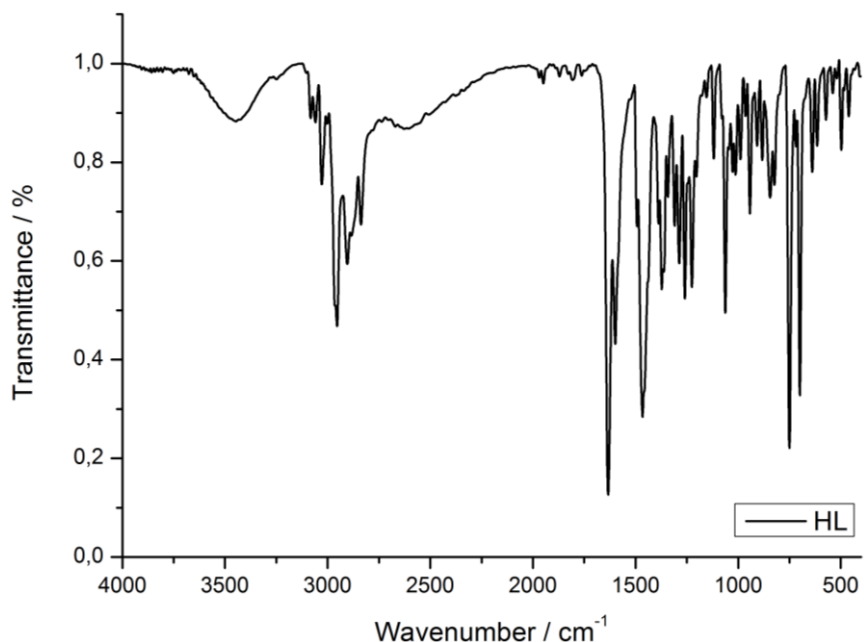


**Figure S1:** FTIR spectrum of **HL** (KBr pellet).

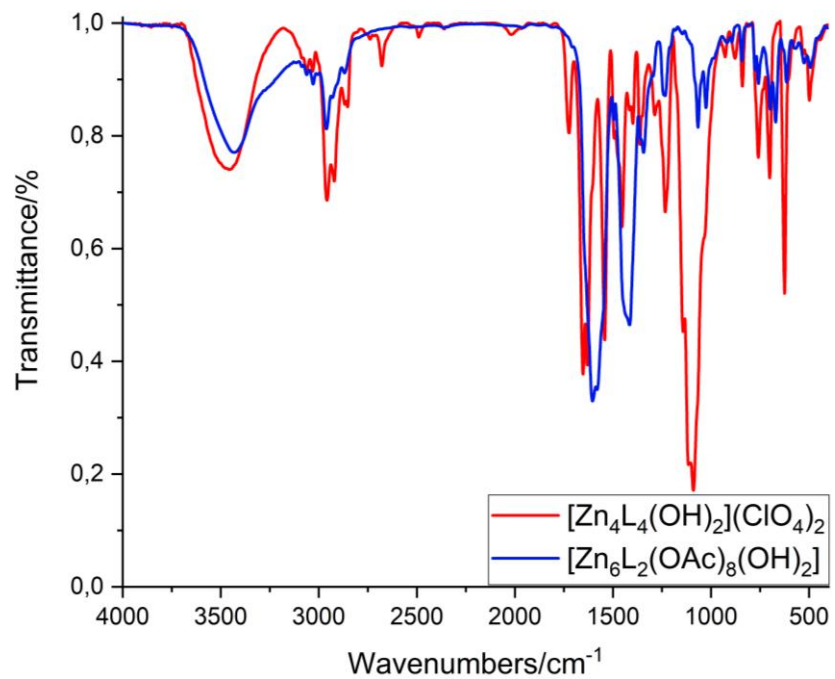


**Figure S2:** FTIR spectra of [Zn<sub>6</sub>L<sub>2</sub>(OH)<sub>2</sub>(OAc)<sub>8</sub>] (**1**, KBr pellet) and [Zn<sub>4</sub>L<sub>4</sub>(OH)<sub>2</sub>](ClO<sub>4</sub>)<sub>2</sub> (**2**, KBr pellet).

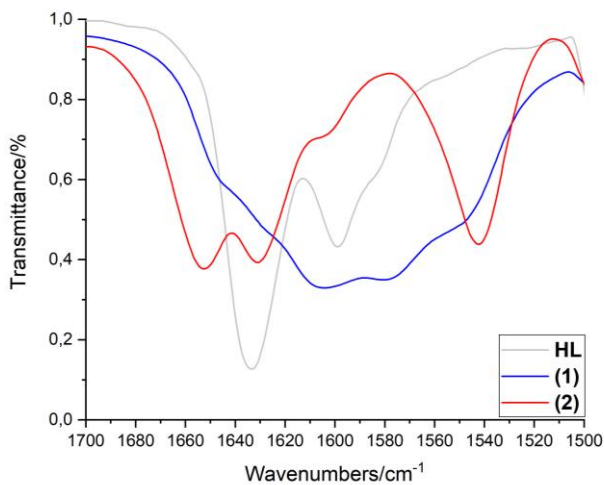


**Figure S3.** Overlay of the FTIR spectra of the ligand (**HL**) and the zinc complexes **1** and **2** (1700-1500 cm<sup>-1</sup>).

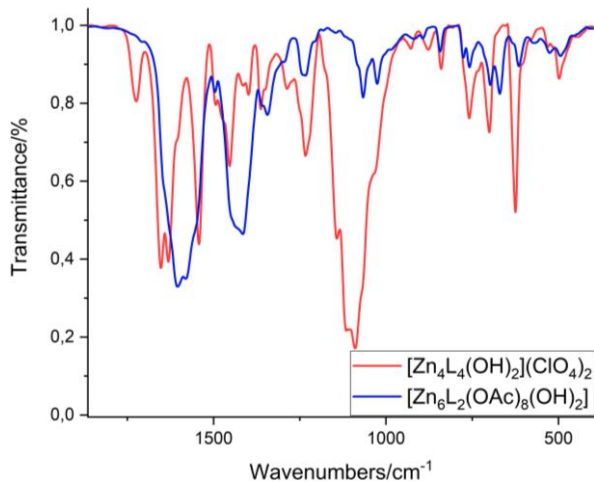


**Figure S4.** Overlay of the FTIR spectra of the zinc complexes **1** and **2** (1750-450 cm<sup>-1</sup>).  
2)

## 2. Packing diagram for **HL**.

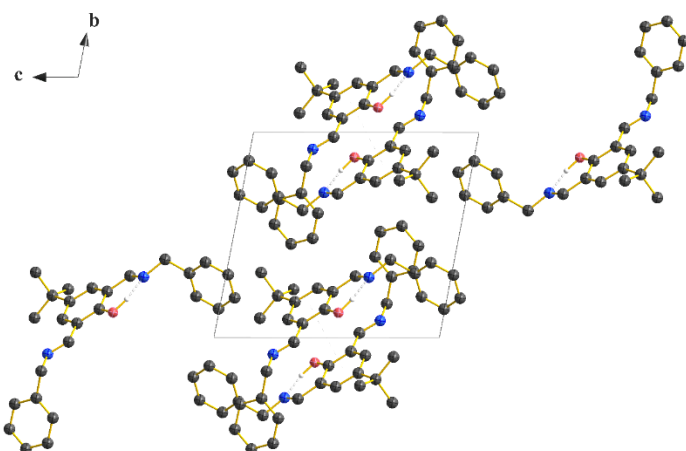


**Figure S5:** Packing diagram of **HL** showing intermolecular  $\pi$ - $\pi$  stacking (offset face-to-face) interactions between adjacent ligand molecules.

### 3. Determination of Coordination Geometries utilizing SHAPE

The coordination geometries of the zinc complexes were examined utilizing the SHAPE program. According to SHAPE, deviations from ideal coordination geometry are represented by a symmetry factor, that increases upon increasing distortions from the ideal geometry, for which the deviation factor is zero.

**Table S1. Shape symmetry factors for complex 1**

Six-Coordinated Zinc atoms in **1** (Zn1, Zn4) -----

HP-6	1 D6h	Hexagon
PPY-6	2 C5v	Pentagonal pyramid
OC-6	3 Oh	Octahedron
TPR-6	4 D3h	Trigonal prism
JPPY-6	5 C5v	Johnson pentagonal pyramid J2

Structure [ML6 ]	HP-6	PPY-6	OC-6	TPR-6	JPPY-6
Zn1 ,	31.959,	24.957,	0.828,	13.389,	28.438
Zn4 ,	31.206,	25.671,	0.721,	13.226,	29.216

Five-Coordinated Zinc atoms in **1** (Zn2, Zn5) -----

PP-5	1 D5h	Pentagon
vOC-5	2 C4v	Vacant octahedron
TBPY-5	3 D3h	Trigonal bipyramidal
SPY-5	4 C4v	Spherical square pyramid
JTBPY-5	5 D3h	Johnson trigonal bipyramidal J12

Structure [ML5 ]	PP-5	vOC-5	TBPY-5	SPY-5	JTBPY-5
Zn2 ,	29.426,	1.717,	4.444,	0.440,	6.940
Zn5 ,	31.065,	3.507,	1.552,	1.849,	4.376

Four-Coordinated Zinc atoms in **1** (Zn3, Zn6) -----

SP-4	1 D4h	Square
T-4	2 Td	Tetrahedron
SS-4	3 C2v	Seesaw
vTBPY-4	4 C3v	Vacant trigonal bipyramidal

Structure [ML4 ]	SP-4	T-4	SS-4	vTBPY-4
Zn3 ,	28.540,	0.502,	6.311,	2.797
Zn6 ,	29.538,	0.350,	6.655,	3.021

### Shape symmetry factors for complex 2

Zn-Polyeder

PP-5	1 D5h	Pentagon
------	-------	----------

vOC-5	2 C4v	Vacant octahedron
TBPY-5	3 D3h	Trigonal bipyramidal
SPY-5	4 C4v	Spherical square pyramid
JTBPY-5	5 D3h	Johnson trigonal bipyramidal J12

Structure [ML5 ]	PP-5	vOC-5	TBPY-5	SPY-5	JTBPY-5
Zn1	, 28.490,	5.477,	2.372,	3.635,	4.374
Zn2	, 31.065,	3.507,	1.552,	1.849,	4.376
Zn3	, 28.969,	5.073,	2.693,	3.047,	4.619
Zn4	, 29.457,	5.271,	2.085,	3.327,	4.307

#### 4. Characterization of compounds - NMR spectroscopy

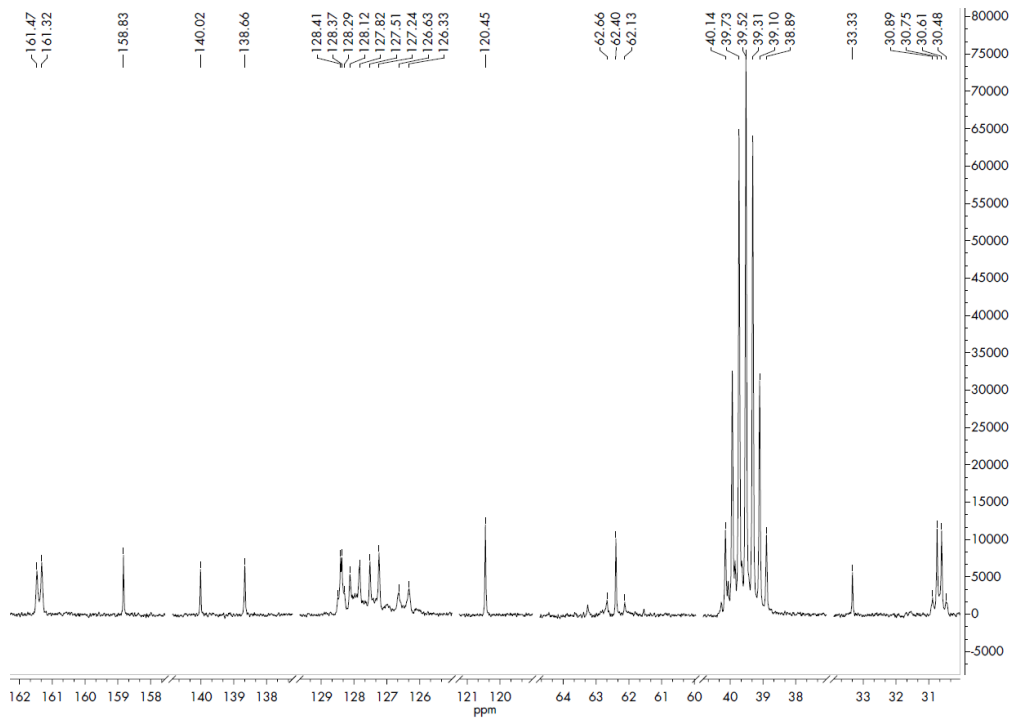


**Figure S6:**  $^{13}\text{C}$ -NMR spectrum of **HL** recorded in dimethylsulfoxide- $d^6$  at 363 K; multiplicity of C-H coupling displayed; parts of the spectrum without signals cut out for better observation of the multiplicities.

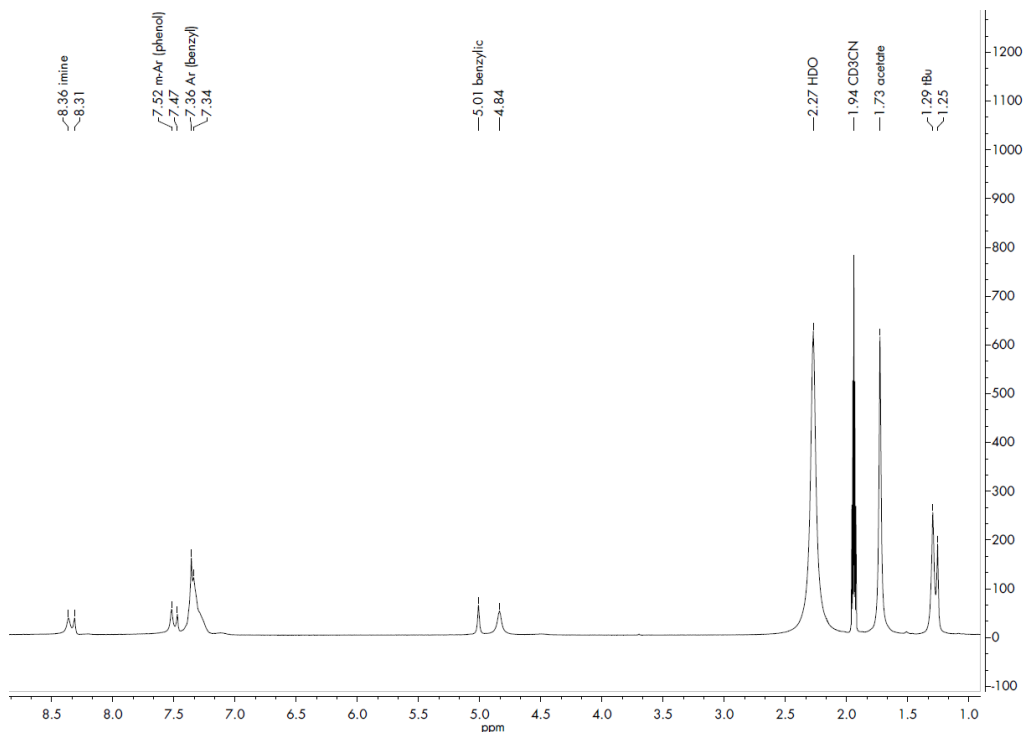


**Figure S7:**  $^1\text{H}$ -NMR spectrum of  $[\text{Zn}_6\text{L}_2(\text{OH})_2(\text{OAc})_8]$  recorded in  $\text{CD}_3\text{CN}$  at ambient temperature.

## 5. UV-vis spectroscopy & Fluorescence spectroscopy

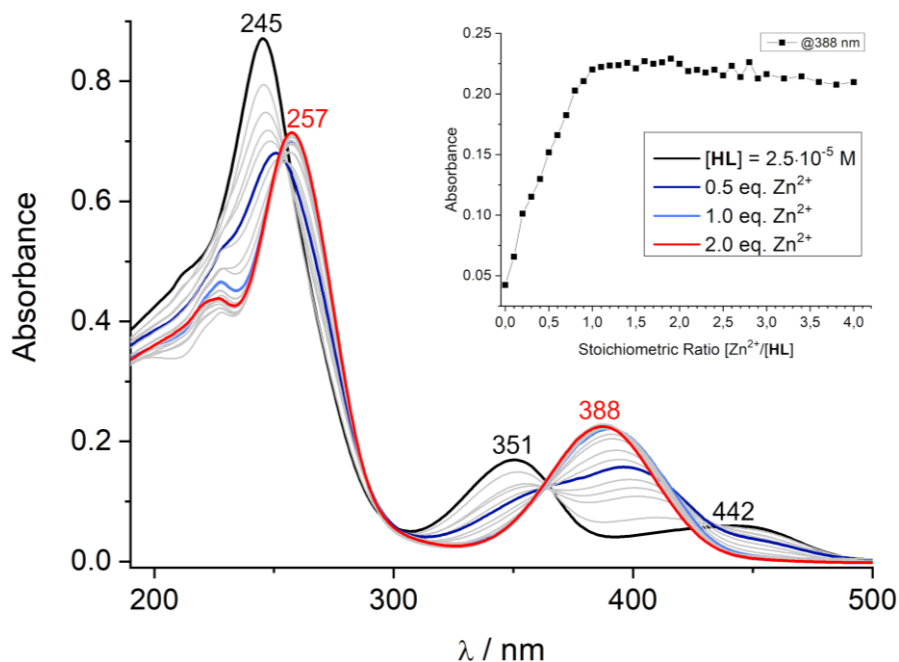


**Figure S8.** Spectrophotometric titration of **HL** with  $\text{Zn}(\text{ClO}_4)_2 \cdot 6 \text{ H}_2\text{O}$  in  $\text{CH}_2\text{Cl}_2/\text{MeOH}$  (3:2/v:v) at a  $10^{-5}$  M concentration and constant ionic strength ( $10^{-2}$  M  $\text{N}(n\text{-Bu})_4\text{PF}_6$ ,  $T = 295$  K). The blue curve corresponds to a final  $\text{Zn}^{2+}/\text{HL}$  molar ratio of 1:1. The inset shows the evolution of selected absorbance values versus the  $[\text{Zn}^{2+}]/[\text{HL}]$  molar ratio.

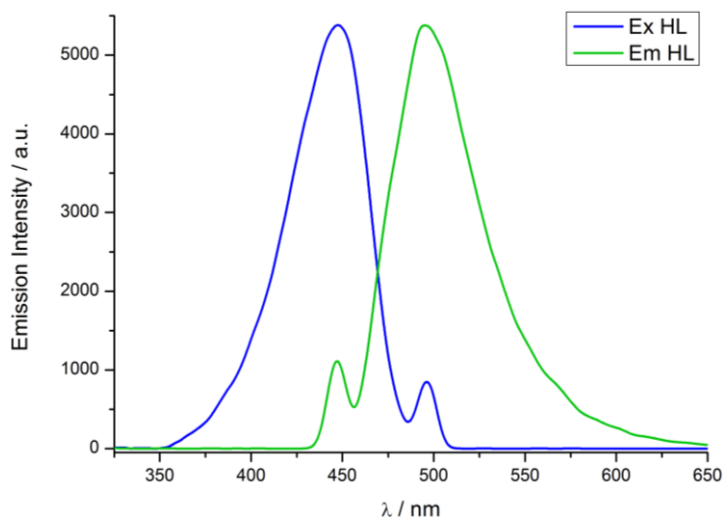


**Figure S9.** Excitation (blue) and emission spectrum (green) of **HL** in acetonitrile ( $c(\text{HL}) = 1 \cdot 10^{-5} \text{ M}$ , 298 K). MeCN;  $c(\text{NEt}_3) = 1 \cdot 10^{-5} \text{ M}$ ;  $\lambda_{\text{Ex}} = 447 \text{ nm}$ ;  $\lambda_{\text{Em}} = 497 \text{ nm}$

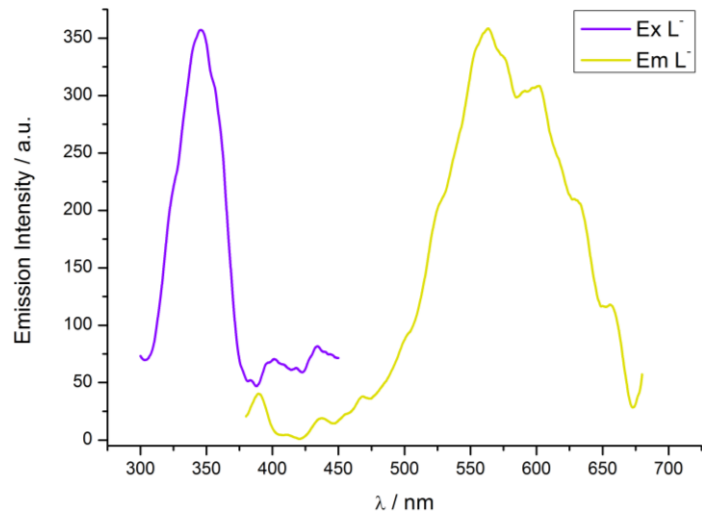


**Figure S10:** Excitation (violet) and emission spectrum (yellow) of **L<sup>-</sup>** in acetonitrile in the presence of base ( $c(\text{HL}) = 1 \cdot 10^{-5} \text{ M}$ ,  $c(\text{NEt}_3) = 1 \cdot 10^{-5} \text{ M}$ , 298 K). MeCN;  $c(\text{HL}) = 1 \cdot 10^{-5} \text{ M}$ ;  $c(\text{NEt}_3) = 1 \cdot 10^{-5} \text{ M}$ ;  $\lambda_{\text{Ex}} = 346 \text{ nm}$ ;  $\lambda_{\text{Em}} = 563 \text{ nm}$

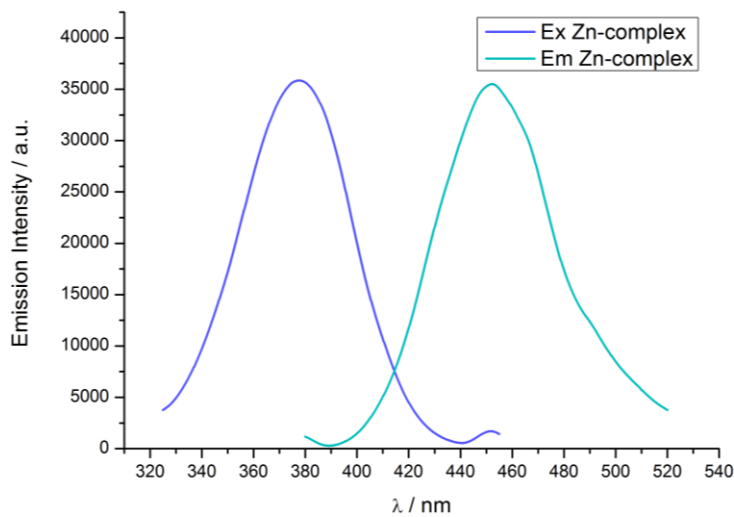
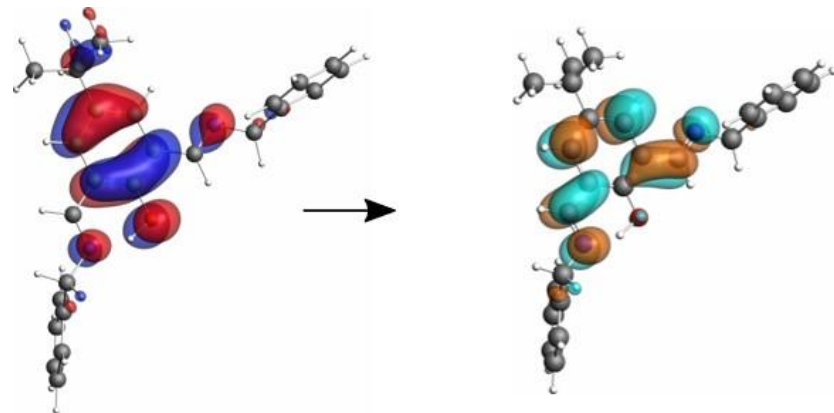


**Figure S11.** Excitation (azure) and emission spectrum (turquoise) of  $[\text{Zn}_6\text{L}_2(\text{OH})_2(\text{OAc})_8]$  in acetonitrile ( $c(\text{complex}) = 1 \cdot 10^{-5}$  M, 298 K).  $\lambda_{\text{Ex}} = 378$  nm;  $\lambda_{\text{Em}} = 452$  nm.

## 6. Characterization of compounds – DFT calculations

a)



b)

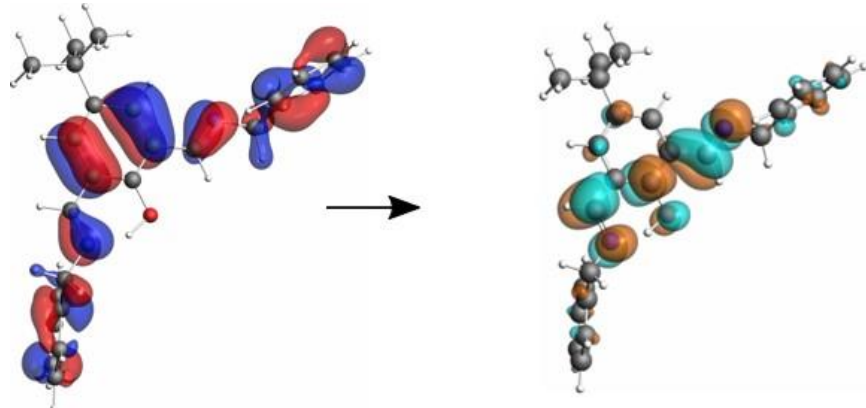
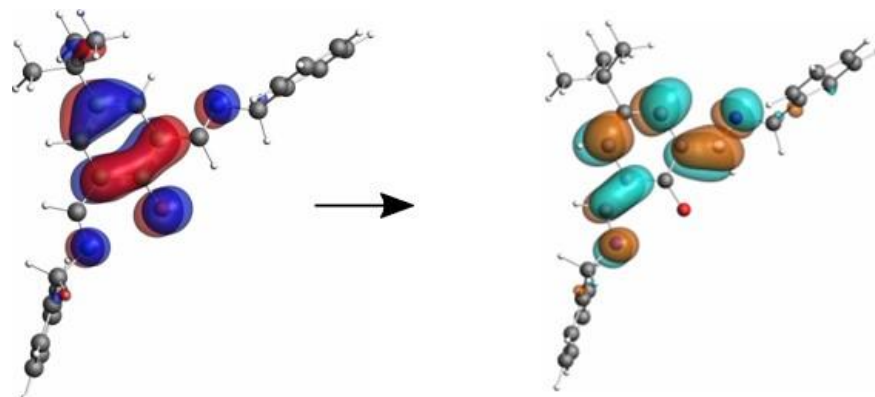


**Figure S12:** Major contributions to the observed UV-Vis bands of **HL** with the single orbital transition contribution in parentheses. a) HOMO $\rightarrow$ LUMO: 334 nm (97%). b) HOMO-1 $\rightarrow$ LUMO+1: 245 nm (67%).

a)



b)

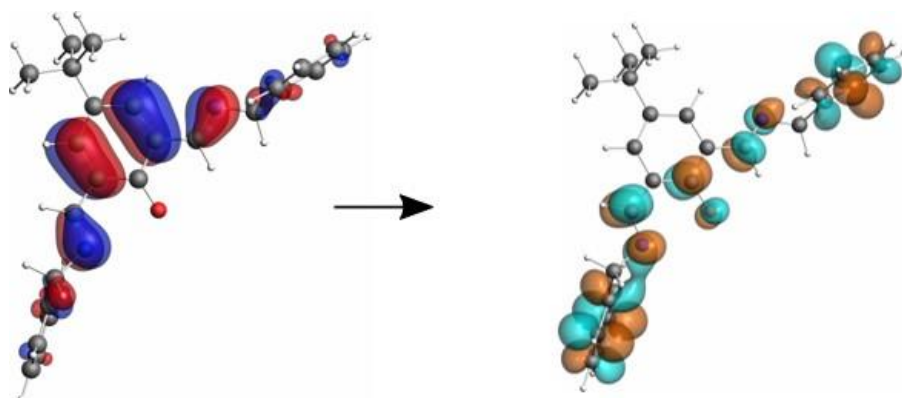


**Figure S13:** Major contributions to the observed UV-Vis bands of  $\text{HL}^-$  with the single orbital transition contribution in parentheses. a)  $\text{HOMO} \rightarrow \text{LUMO}$ : 409 nm (98%). b)  $\text{HOMO-2} \rightarrow \text{LUMO+1}$ : 229 nm (36%).

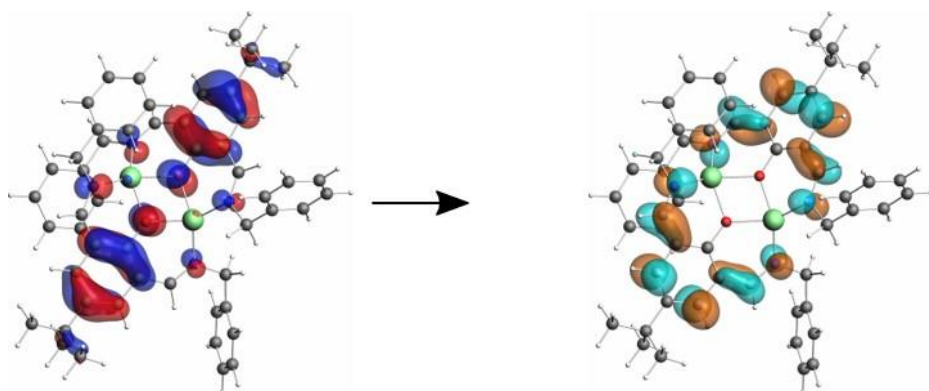


**Figure S14:** Major contributions to the observed UV-Vis bands of  $[\text{Zn}_2\text{L}_2]^{2+}$  with the single orbital transition contribution in parentheses. a)  $\text{HOMO} \rightarrow \text{LUMO}$ : 348 nm (57%).

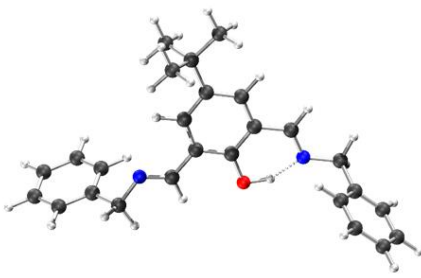


**Figure S15:** PBE-D3(BJ) optimized structure of **HL** used for the simulation of UV-Vis spectra (pristine) and basis for the other used structures.

Calculated atomic coordinates have been deposited at the open access data base zenode, see  
<https://doi.org/10.5281/zenodo.7837334>

## 7. Determination of detection limit (LOD value)

The fluorescence intensity of **HL** at 454 nm as a function of the  $\text{Zn}^{2+}$  ion concentration was found to be linear in the range from  $1 \cdot 10^{-6}$  to  $1 \cdot 10^{-7}$  M. The limit of detection (c<sub>LOD</sub> value; c<sub>LOD</sub> =  $3\sigma_{\text{bl}}/b$ , where  $\sigma_{\text{bl}}$  is the standard deviation of the blank measurements and b the slope of the regression line according to the IUPAC definition)) is a measure for the lowest concentration that can be measured. The fluorescence titration carried out between **HL** and  $\text{Zn}^{2+}$  provides a value of 0.24(4) ppm.

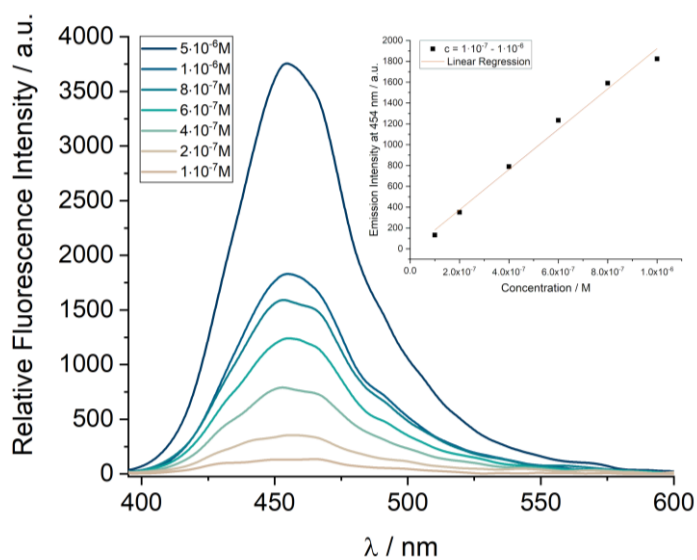


**Figure S16:** Fluorescence spectra **HL** as a function of  $\text{Zn}^{2+}$  ion concentration.